

Abaya Geothermal Project, A High Enthalpy Geothermal System in the Main Ethiopian Rift

Snorri Gudbrandsson, Chelsea Cervantes, Hjálmar Eysteinnsson and Gestur Gíslason
Reykjavík Geothermal

Keywords

East African Rift, Ethiopia, Main Ethiopian Rift, SMER, Abaya, High Enthalpy, Surface exploration

ABSTRACT

The Abaya geothermal project is located on the western flank of the Southern Main Ethiopian Rift (SMER), where the plateau transitions into the rift floor, and is the southernmost of Reykjavík Geothermal's (RG) projects in Ethiopia. The concession is directly north of Lake Abaya, in what is known as the Southern Nations, Nationalities and Peoples' Region (SNNPR) and is located approximately 280 km southwest from the country's capital, Addis Ababa.

The western half of the concession is bisected by a NNE-SSW trending fault swarm and the concession is also the setting for three graben structures, the Salewa Dore - Hako Graben, which is thought to host an array of scoria cones and active fissures, the Abaya Graben, and the Chewkare Graben. Surrounding and within the license area are various volcanic centers known as Doguna, Salewa-Dore, Hako, Chericha, and Donga. The Salewa-Dore and Hako rhyolitic complex is thought to accommodate the most recent volcanic activity in the area, with several minor geothermal manifestations. Most geothermal surface manifestations are found on the Abaya fault, a large ignimbrite escarpment on the western part of the Abaya Graben. These manifestations are both thermal springs, ranging from moderate 35 °C to boiling as well as steaming ground/fumarolic activity, at close to 100 °C at 20 cm depth.

Through numerous and extensive field campaigns, RG has been compiling GIS, geological, geochemical and geophysical data of the Abaya geothermal prospect in the aim of creating a scientific foundation to characterize the geothermal production potential of the area. Geochemical sampling of thermal manifestations, subsurface fault characterization, rock sampling, soil-gas analysis and a MT/TEM survey provide the data to create a conceptual model. Collected data suggests the Abaya region to be a high-enthalpy geothermal prospect.

1. Introduction

Reykjavík Geothermal is an Icelandic geothermal development company that has been active in Ethiopia since 2011. Prior to the Abaya geothermal project, RG has been instrumental in the Corbetti geothermal project and Tulu Moye geothermal project, both located the Main Ethiopian Rift. The Corbetti and Tulu Moye projects have signed a Power Purchase agreement with the Government of Ethiopia for 520 MWe, each. Abaya is therefore the third area that RG is investigating in Ethiopia.

Reykjavík Geothermal (RG) has carried out geothermal surface exploration in the Abaya high temperature prospect in Ethiopia. The concession is located about 280 km southwest of the capital city Addis Ababa in the Main Ethiopian Rift (MER), as measured from Google Earth, and is part of the East African Rift System (EARS). The concession area is 513 km² (2019) and is labelled in *Figure 1*, along with two other RG geothermal concessions: Tulu Moye and Corbetti.

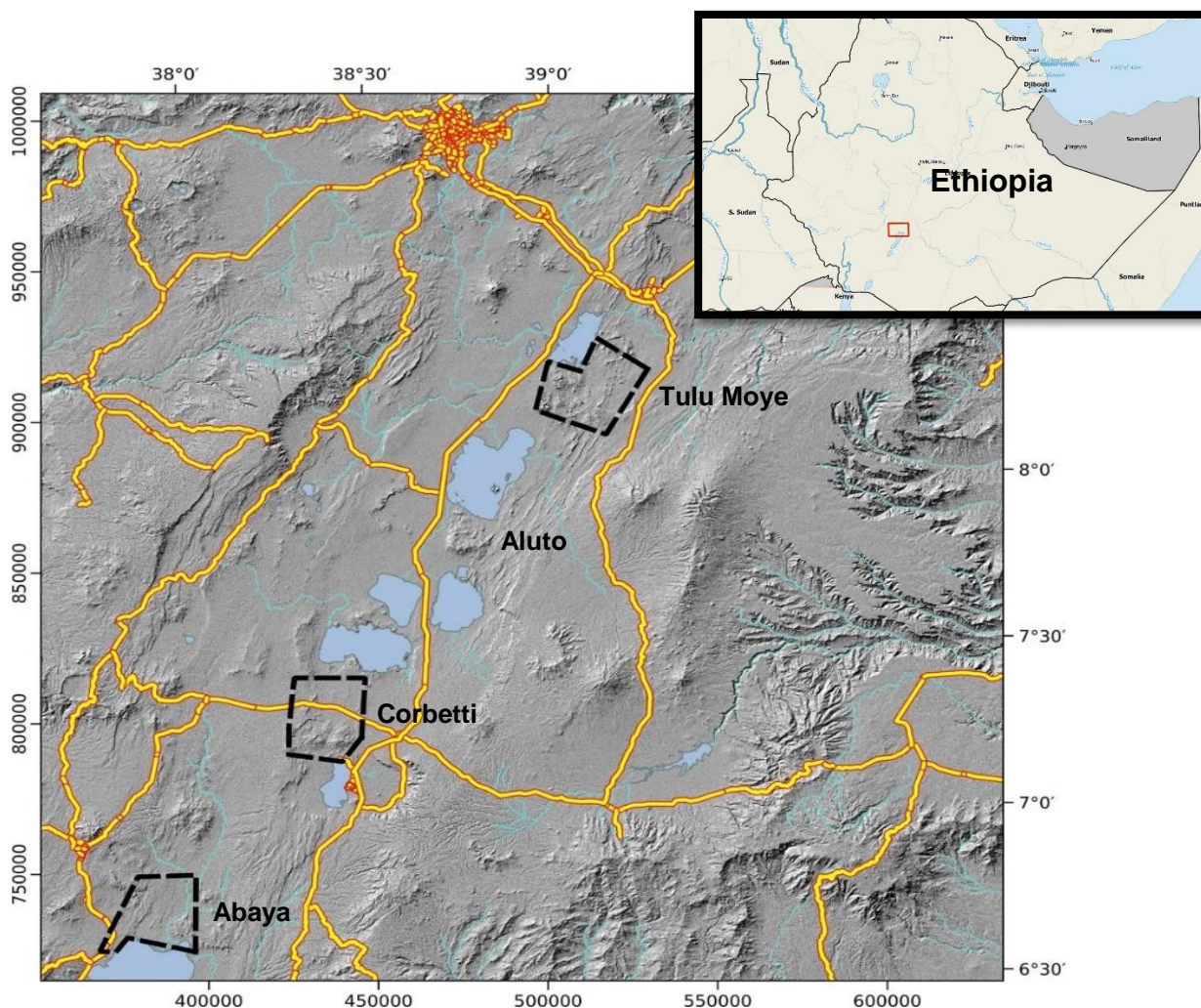


Figure 1: The Reykjavík Geothermal concessions in Ethiopia. The reference map in the upper right-hand corner shows the location of the Abaya concession.

2. Surface Exploration

2.1 Geology

The Main Ethiopian Rift (MER) is part of the Great East African rift system running generally in NNE-SSW direction. It extends from Lake Chamo in the south and to the north in the vicinity of Dofan volcano. It is bounded on both sides by high rising plateaus (2500 m a.s.l.) with the lowest part being the rifting floor in between. The initial stage of the formation of the rift system dates back to early Tertiary (Upper Eocene) where initial uplift of the Afro Arabian dome took place centred in the Afar triple junction (Mohr, 1971). This was followed by fissural eruption of extensive flood basalt volcanism, of alkali to transitional composition, known as the Trap Series. This episode was followed by extensional tectonism, which resulted in the thinning of the crust that led to the formation of the Ethiopian Rift valley.

The Abaya area is located in the western margin of the Southern Main Ethiopian Rift (SMER), which extends from Lake Hawassa until Lake Chamo. The local geology of the region consists of both igneous and sedimentary rocks. The rift floor is comprised of Tertiary-aged ignimbrite, commonly known as the Chewkare Ignimbrites, which are exposed especially in the area of the northwest Abaya fault (Ayele, Teklamariam, & Kebede, 2002; Corti et al., 2013). When not exposed in outcrops, the ignimbrite is otherwise overlain by lava flows originating from the many felsic eruptive centers present in the area. Alluvial and fluvial sedimentary deposits are Pleistocene – Holocene in age (Chernet, 2011). These deposits originate both from large lakes that existed in the Pleistocene, and from the more recent influence of Lake Abaya (Ayele et al., 2002; Corti et al., 2013).

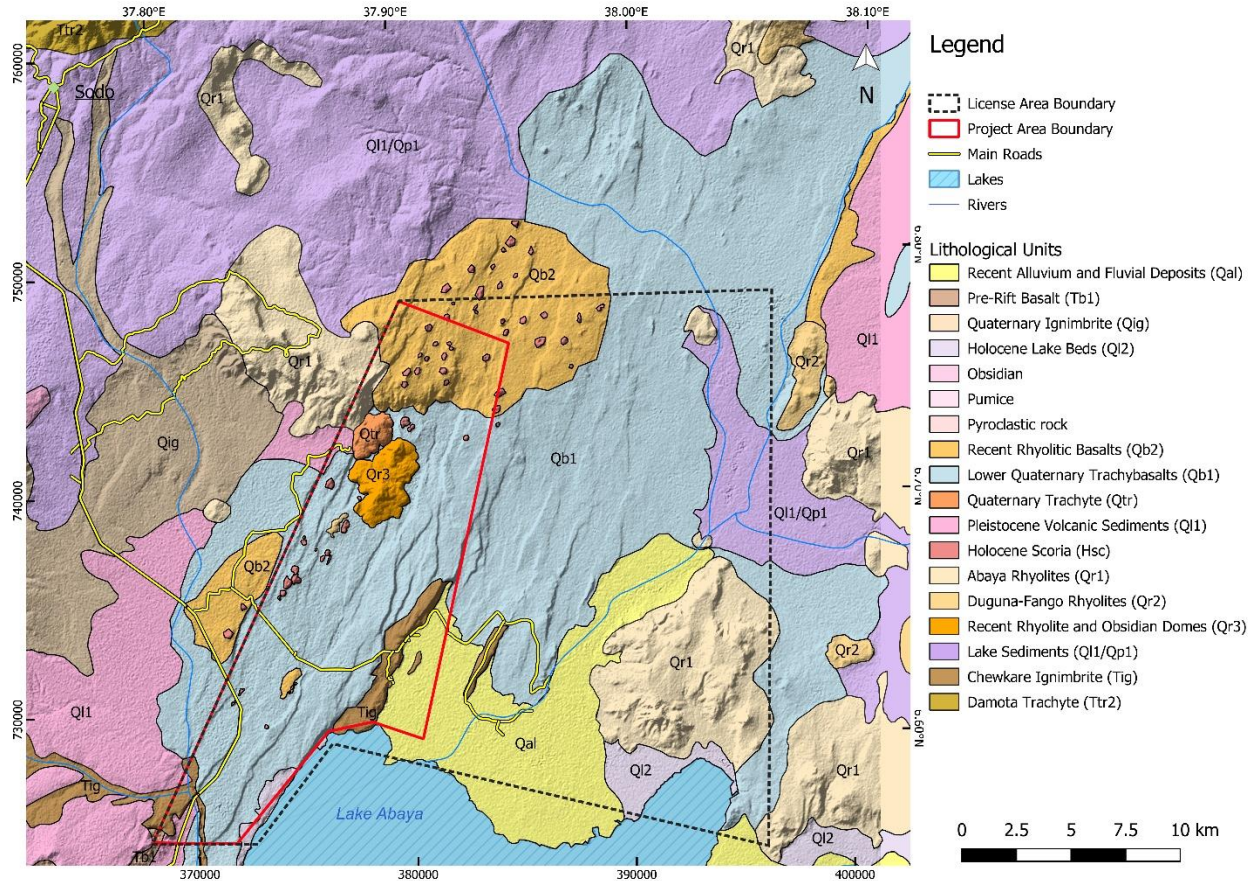


Figure 2 Geological Map of the Abaya concession. Modified from Chernet (2011)

2.2 Structure

The last stage of the volcano – tectonic activity took place during Pleistocene to present in the MER and is related to the axial extensional zone denoted as the Wonji Fault Belt (WFB), resulting in bimodal basalts and rhyolitic volcanic products accumulated on the rift floor (Chernet, 2011). The WFB is arranged in an “en-echelon” feature, which is a typical phenomenon of the Rift (Di Paola, 1970; Electroconsult (ELC), 1987). The activity resulted in the formation of NNE-SSW trending series of faults shattering the rift floor creating rift in rift structures, and producing step like structures and volcanism (Wonji Group) (Mohr, 1971). Some of the felsic products of this tectonic activity in the Abaya region are the volcanic complexes of Duguna-Fango, Obitcha, Salewa Dore, Hako, Kilisa and Donga, which rest on the southernmost section of the WFB (Chernet, 2011).

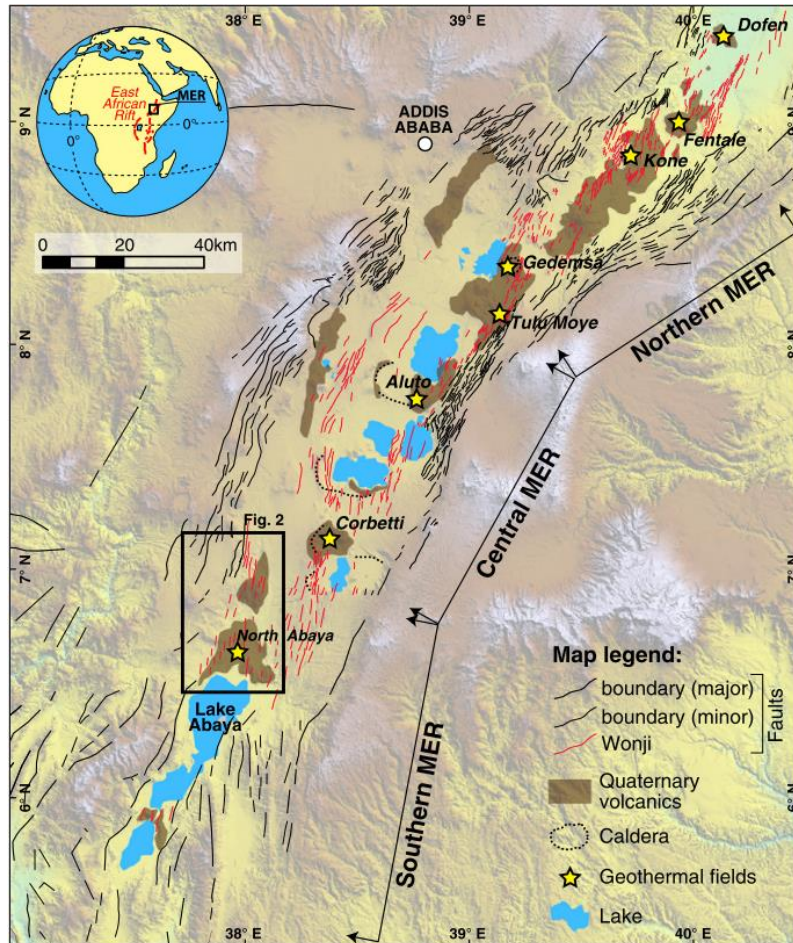


Figure 3: Tectonic map of the MER. The Wonji Fault Belt and the boundary faults can be observed. The black box indicates the location of the Abaya geothermal prospect. Source: Minissale (2017)

The SMER is thought to be comprised of less-evolved rifting in comparison to the Central and Northern MER (Corti et al., 2013). The tectonic history of the SMER began in the late Miocene with regional extensional tectonics and subsidence (Chernet, 2011). This was followed in the Pliocene by rift-margin rhyolitic volcanism, producing extensive ignimbrite successions and trachytic volcanism in the rift-shoulders (Chernet, 2011). The area is characterized by the absence of a major rift escarpment as might be expected from a rift margin setting, and instead the topographic transition is gentle between the rift floor and plateau (Minissale et al., 2017).

The Abaya region is the setting for the Obitcha caldera, an oval-shaped structure that spans approximately 16 km at its widest expanse. Intersecting this caldera starting from further southwest is a NNE-SSW fault swarm that encompasses the western Abaya region, in the transitional zone between the rift shoulder and the rift floor. The numerous normal faults are closely spaced, have limited vertical offset and often present themselves in an en-echelon pattern, as seen below in *Figure 4* (Corti et al., 2013). Major thermal manifestations are found in the area of the northwest Abaya fault, located above the northwest corner of Lake Abaya. The base of the fault scarp strikes NNE-SSW and is believed to have a dip of 75-80° to the east (Ayele et al., 2002;

Mamo & Abteu, 2008). The dominant N-S to N20° fault direction in the western boundary of the rift is homogeneous to the WFB, however, it is not consensus within scientific literature as to whether the fault swarm in the western Abaya region is classified as an extension of the WFB, or rather an en-echelon faults associated with a horizontal displacement between the Gofa basin southwest of the area and the Galana basin southeast of the area. As the Abaya concession is located in a transition zone between the western rift shoulder and the rift floor, it may be that the faulting of the area is indeed characterized more by boundary faulting, rather than Wonji faulting. Lastly, there are three inferred graben structures that trend NE-SW in the Abaya region: the Salewa Dore – Hako, Abaya, and Chewkare Graben. The Salewa Dore – Hako Graben hosts an array of scoria cones that appear within the graben and scatter towards the NE. The western margin of the Abaya Graben (northwestern Abaya fault) hosts the most prominent surface manifestations in the area.

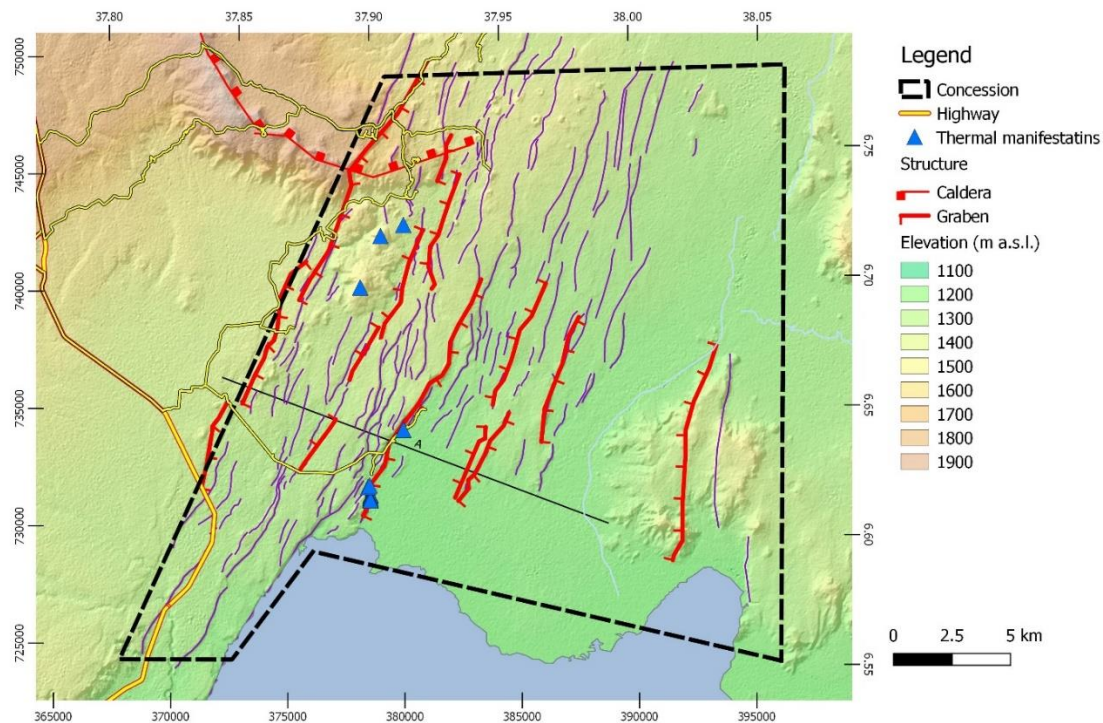


Figure 4: A structural map of the area. Surface manifestations (blue triangles) are found around Salewa Dore – Hako rhyolitic complex and the Abaya Fault. The cross section (A) is displayed in Figure 5.

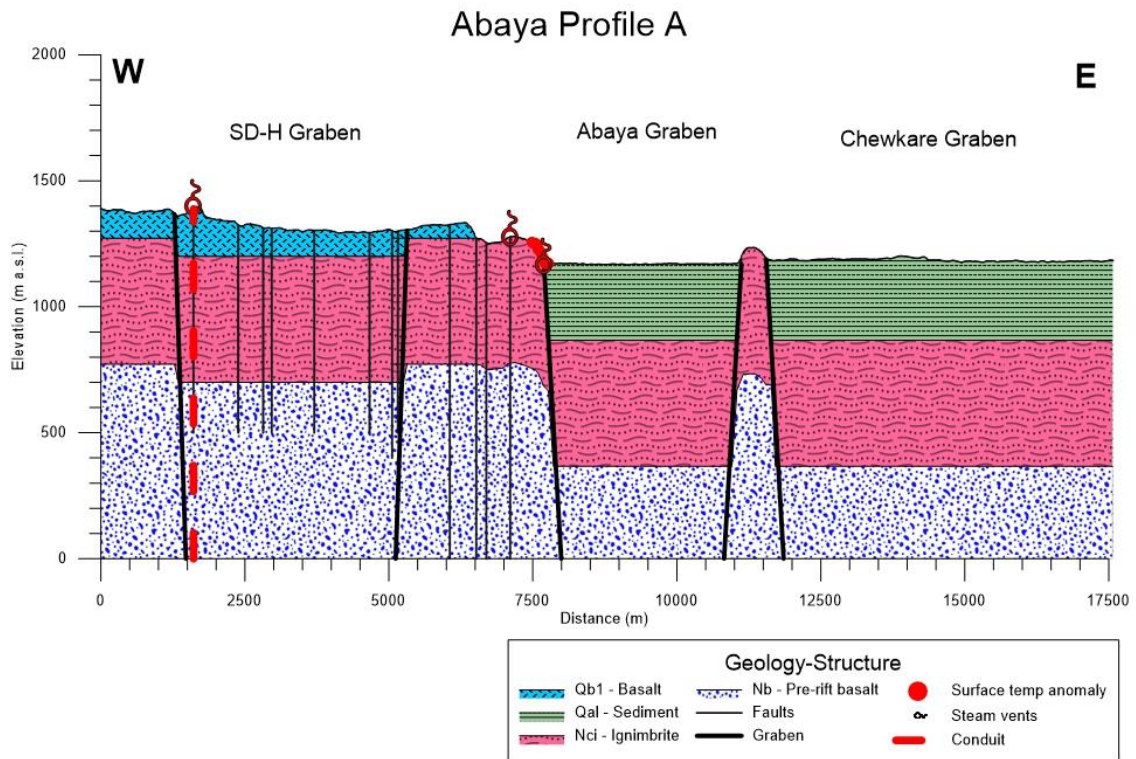


Figure 5: A W-E cross-section over the eastern flank of the SMER. The three distinct grabens, SD-H Graben, Abaya Graben and Chewkare Graben, from west to east. Geothermal surface manifestations are observed in the SD-H Graben on the rhyolitic complex and in the Abaya Fault on the western flank of the Abaya Graben.

2.3 Geochemistry

Several field surveys have taken place in the Abaya region, collecting samples in and around the geothermal license of Reykjavík Geothermal. The chemical composition of the spring water has been published both in technical reports, (Electroconsult (ELC), 1987), Ayele et al. (2002), Berhanu Gisaw (2007) (Personal communication) and Reykjavík Geothermal reconnaissance 2011. No gas chemistry from the area has been found in literature by RG.

2.3.1 Water Chemistry

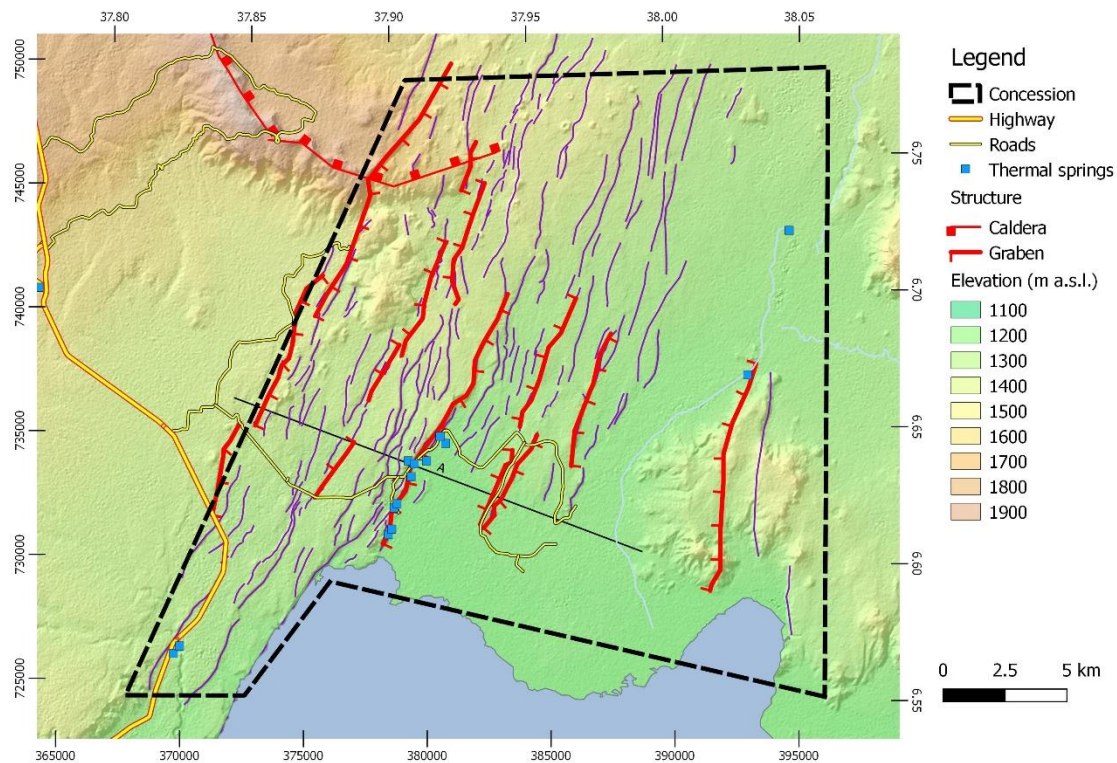


Figure 6: A structural map of the area. Surface manifestations (blue squares) are found around the Abaya Fault.

Reykjavík Geothermal collected gas and water samples on two field excursions in 2018 and 2019 from springs and fumaroles in the area. The geothermal manifestations in Abaya are found in two areas: around the Salewa Dore – Hako rhyolitic complex where several weak, moderate-temperature steaming spots are found at 30-45 °C, and on the Abaya fault, northwest of Lake Abaya where springs, boiling mud pools and fumaroles are found with temperature ranging from 50 – 100 °C.

Along the Abaya fault and on the western side of a small horst several springs and hydrothermally altered surface rocks with weak fumarolic activity are found. The springs range in temperature from 40 °C to close to 100 °C, with heat increasing from north to south.

The chemical composition from all sampled springs are presented in *Table 1*. The waters collected from the springs (labelled as Sp-XX) show high SiO_2 , from 107 in Sp-2 to 512 ppm in Sp-6, high CO_2 concentration and relatively low SO_4 (1-155 ppm), and chlorine (2-815 ppm). As shown in *Figure 7*, the anion ternary diagram plots all water samples as peripheral water, with only one water sample suggested to be steam heated. In this case the high CO_2 concentrations and lack of H_2S , as observed also in the Corbetti and Tulu Moye RG concessions, might eschew the characteristics of the water, plotting them as peripheral waters. The silica concentration and temperature increase from north to south with springs 5 and 6 showing both highest SiO_2 concentration as well as the highest temperatures.

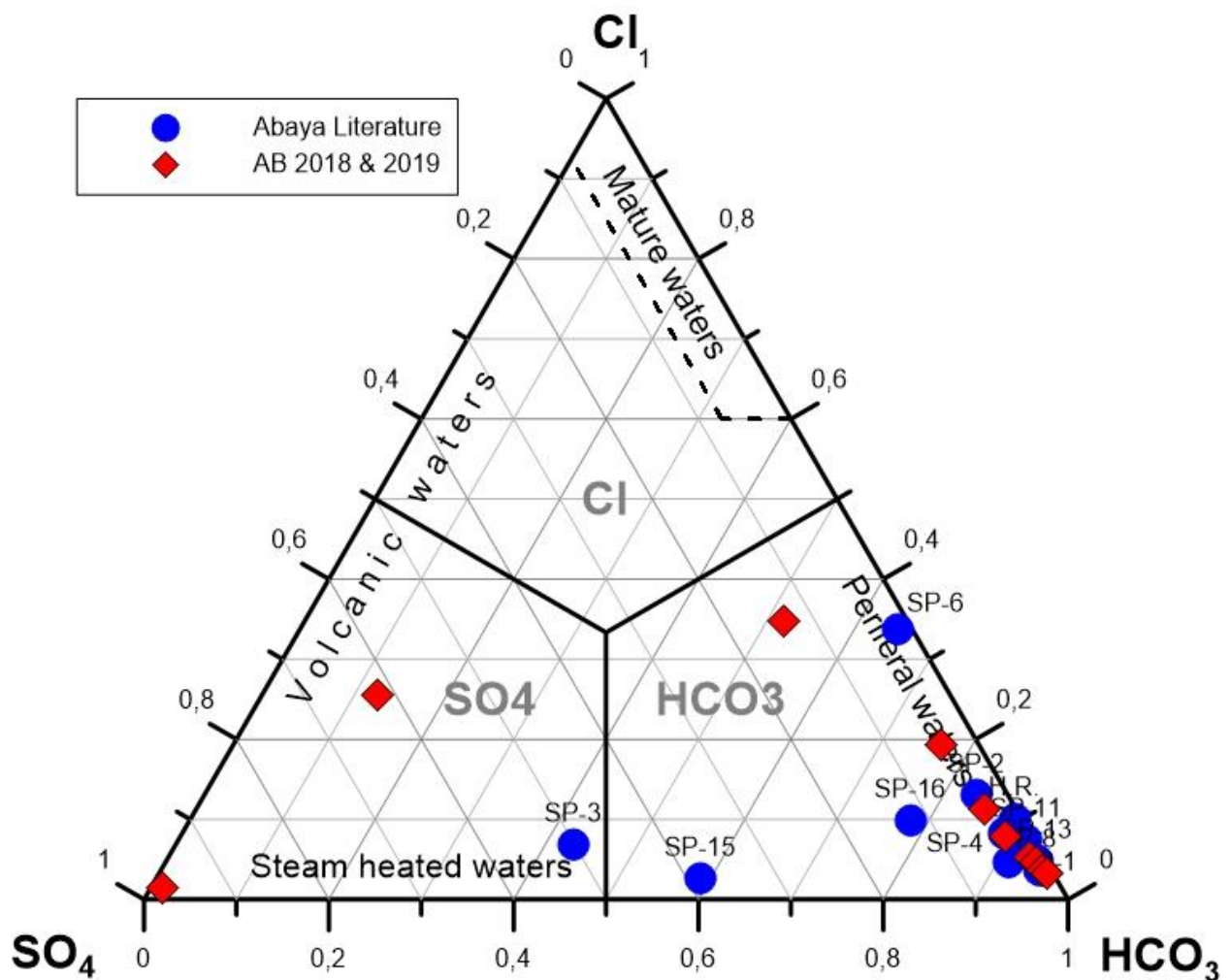


Figure 7: An anion diagram of the waters sampled from the springs in Abaya. All waters, apart from one, are suggested to be surface waters with CO_2 dominant species.

Table 1. Chemical composition of water samples from Abaya, in ppm.

Sample ID	pH	T°C	H ₂ S	CO ₂	CO ₃	HCO ₃	SO ₄	Cl	F	Na	K	Ca	Mg	B	SiO ₂	Fetot	As	Al
AbayaL; 2007	8.9	25	N.r.	374.0	23.8	486	19.0	69.0	8.5	240.0	19.0	12.1	3.0	3.0	48.0	N.a.	N.a.	N.a.
SP-1 2000	6.7	34	N.r.	172.4	0.1	170	4.0	8.0	1.6	49.0	9.3	20.0	7.0	0.2	144	N.a.	N.a.	N.a.
SP-2 2000	7.6	39	N.r.	559.0	2.6	723	22.0	104	2.7	223.0	26.0	34.0	40.0	0.0	107	N.a.	N.a.	N.a.
SP-3 2000	6.9	41	N.r.	639.8	0.5	707	24.0	103	2.8	213.0	26.0	53.0	56.0	0.2	123	N.a.	N.a.	N.a.
SP-4 2000	6.4	43	N.r.	996.9	0.2	805	13.0	72.0	15.0	530.0	41.0	16.0	55.0	0.2	155	N.a.	N.a.	N.a.
SP-5 2000	9.5	58	N.r.	1208	417	1250	89.0	762	46.0	1370	174.0	0.2	0.1	3.1	433	N.a.	N.a.	N.a.
SP-6 2011	9.68	21.2	0.1	1173	285	1334	88.5	697	40.8	1280	177.0	0.5	0.2	3.7	512	0.1	996	0.2
SP-8 2011	6.91	24.3	N.d.	1220	1.1	1347	10.8	52.1	13.0	540.0	33.9	19.7	9.9	0.8	151	1.1	67.4	0.1
SP-9 2000	7.9	48	N.r.	486.9	4.7	650	11.0	51.0	20.0	292.0	16.0	6.5	1.8	0.3	150	N.a.	N.a.	N.a.
SP-11 2000	7.5	46	N.r.	488.3	2.0	636	10.0	50.0	20.0	280.0	13.1	6.4	1.5	0.0	128	N.a.	N.a.	N.a.
SP-13 2000	8.2	46	N.r.	598.0	11.7	804.0	9.0	40.0	16.0	342.0	18.1	5.2	3.3	0.4	144	N.a.	N.a.	N.a.
SP-15 2011	7.29	23.7	N.d.	1137.0	2.5	1418	10.7	63.0	13.7	495.0	31.7	16.6	6.5	0.8	144	0.6	58.7	0.1
SP-16 2011	7.56	23.5	N.d.	586.0	2.1	748	17.0	94.5	2.2	206.0	27.4	38.5	44.3	0.6	114	0.0	2.2	0.0
SP-19 1976	7.4	20	2	456.5	1.2	575	11.0	45.0	18.0	280.0	22.0	8.0	7.0	0.3	126	N.a.	N.a.	N.a.
SP-20 1976	7	25	N.d.	437.2	0.4	500	11.0	18.0	12.0	194.0	27.0	16.0	5.0	0.1	112	N.a.	N.a.	N.a.
SP-16 AB-18-W01	6.39	41.4	N.a.	543	0.2	397	21.0	99.7	N.a.	219	30.6	39.4	43.3	0.1	119.1	0.1	N.a.	0.13
SP-15 AB-18-W02	5.94	67	N.a.	949	0.1	423	16.8	55.3	N.a.	524	33.8	18.3	6.0	0.3	138.6	1.4	N.a.	0.38
Spring AB-18-W03	5.4	88.1	N.a.	10.2	0.0	1.4	105	1.6	N.a.	6.0	9.3	2.2	0.5	0.0	116.8	0.1	N.a.	0.06
SP-8 AB-18-W04	6.23	67.3	N.a.	866	0.2	571.4	18.4	50.6	N.a.	493	34.3	19.2	8.4	0.3	147.1	0.2	N.a.	0.17
SP-15 AB-18-W05	5.94	67	N.a.	N.a.	N.a.	N.a.	14.5	54.5	N.a.	533	34.2	16.5	5.9	0.3	142.9	0.1	N.a.	0.07
SP-15 AB-18-W06	6.23	67.3	0.017	1396	0.4	938.5	14.8	52.7	N.a.	527	33.6	16.7	5.6	0.3	142.9	1.3	N.a.	0.19
SP-15b AB-18-W07	6.4	67.7	0.018	1357	0.7	1092	14.2	53.2	N.a.	530	33.7	16.4	5.6	0.3	142.5	1.4	N.a.	0.15
SP-13 AB-18-W08	6.55	56.8	0.092	1730	1.5	1472	11.1	51.8	N.a.	432	51.3	87.6	61.9	0.3	189.1	1.1	N.a.	0.03
SP-8 AB-18-W09	6.84	67.2	0.115	1295	2.3	1397	14.0	53.3	N.a.	522	35.4	19.7	8.7	0.3	149.5	0.5	N.a.	0.12

N.d.: Not detected

N.a.: Not analysed N.r.: Not reported

The concentrations of sodium in the water samples ranges from 5 to 1370 ppm, potassium 3-174 ppm, calcium 0.4 to 53 ppm and magnesium 0.1 – 56 ppm. The Giggenbach ternary diagram and therefore the geothermometers suggest most spring water to be immature and or partially equilibrated waters but samples collected from spring 5 and 6 suggest partially to fully equilibrated water and reservoir temperatures exceeding 200 °C, as seen in *Figure 8* (Giggenbach, 1988).

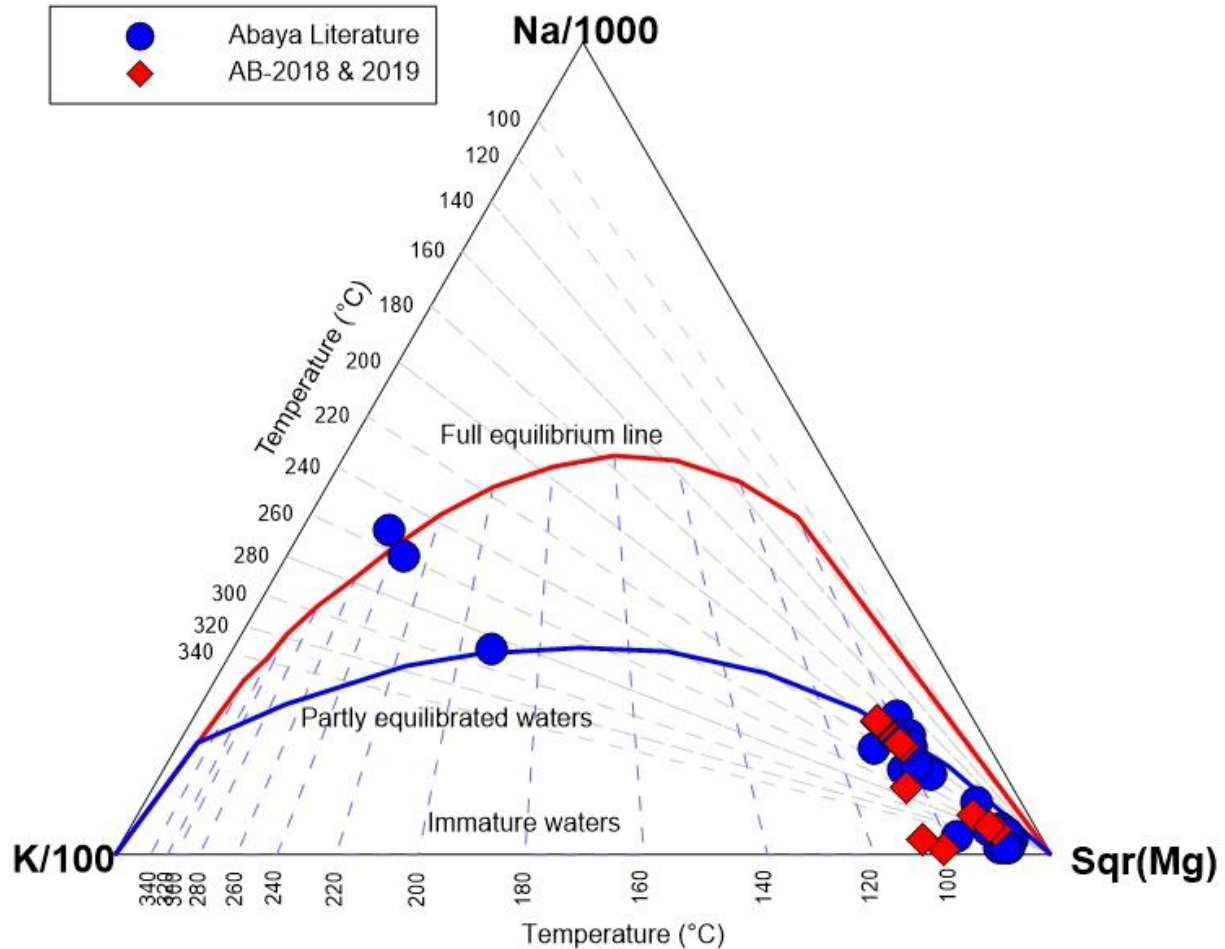


Figure 8: A Giggenbach diagram suggests most water samples collected in the area are of unequilibrated to partially equilibrated waters. Samples collected from Spring 5 and spring 6 show water of partially to fully equilibrated waters with reservoir temperature > 200 °C.

The chemical geothermometers based on water chemistry show high temperatures from all samples, shown in *Table 4*. This is somewhat expected with the cation geothermometers in regard to immature waters due high sodium concentration. The high silica concentration measured in all springs results in estimated reservoir temperature of >140 °C. The highest silica temperature estimation is in agreement with the highest cation reservoir estimated temperature from samples collected from Spring 6, which both show a reservoir temperature estimation of 260 °C. The results of Spring 5 are close to a match, with the silica temperature estimation at 243 °C and cation estimated temperature at 252°C. Because of this, it is inferred that Spring 5 is likely the same location as Spring 6.

Table 2. Reservoir temperature based on the Giggenbach Cation geothermometer. Spring 5 is likely the same location as Spring 6.

	Sample year	Literature		Current study	
		T °C (QTZ)	T °C (Na/K)	T °C (QTZ)	T °C (Na/K)
Abaya Lake	2007	101	214		
SP-1	2000	151	289		
SP-2	2000	136	245		
SP-3	2000	143	249		
SP-4	2000	154	213		
SP-5	2000	216	252		
SP-6	2011	227	260	262	260
SP-8	2011	153	198	164	203
SP-9	2000	153	188		
SP-11	2000	145	178		
SP-13	2000	151	186		
SP-15	2011	151	199	150	199
SP-16	2011	139	256	141	260
SP-19	1976	144	214		
SP-20	1976	138	260		
Spring				146	619

The water geothermometers are applied from Arnorsson et al. (2000). The chemical concentrations are in mg/kgw (ppm):

$$T \text{ } ^\circ\text{C} = \frac{1522}{5.75 - \log \text{SiO}_2} - 273.15 \quad (\text{Fournier, 1977})$$

$$T \text{ } ^\circ\text{C} = \frac{1390}{1.750 + \log\left(\frac{\text{Na}}{\text{K}}\right)} - 273.15 \quad (\text{Giggenbach, 1988})$$

2.3.2 Gas Chemistry

No gas chemistry is available from the area of interest in literature. RG collected several gas samples from weak fumaroles on the southern part of the northwest Abaya fault. These samples were collected in a glass bulb where the H₂S and CO₂ were analysed from the caustic soda in Giggenbach flasks and then further analysed at the Iceland Geosurvey (ISOR) in January 2019.

All samples have very low H₂S concentrations, a trend that has been observed by RG in other Ethiopian geothermal fields, Tulu Moye and Corbetti (in-house reports) and high concentrations of CO₂. The chemical composition of the gases are reported in Table 3.

Table 3. Chemical composition of gas samples collected in Abaya, reported in mmol/kg.

	H ₂ mmol/kg	N ₂ mmol/kg	CH ₄ mmol/kg	O ₂ mmol/kg	Ar mmol/kg	H ₂ S mmol/kg	CO ₂ mmol/kg
AB-19-G04						1.19	11223
AB-19-G05						2.64	72414
AB-19-G06						3.40	106894
AB-19-G02	0.005	1.16	0.543	0.44	0.02	0.14	43560
AB-19-G04	0.005	2.83	0.015	1.37	0.06	0.14	13640
AB-19-G06	0.003	15.8	9.00	5.91	0.33	0.31	93148

Based on the gas concentrations the estimated reservoir heat was calculated using geothermometers from Arnorsson (2000) and thermometers therein. The extremely high CO₂ concentration evidently indicates very high reservoir temperatures, >400 °C. These values are almost certainly too high. The average of the geothermometers, column AVE in *Table 4* suggest reservoir temperatures of >200 °C, which is in good agreement with both SiO₂ thermometers as well as cation thermometers.

Table 4. Calculated estimated reservoir temperatures based on gas composition using geothermometers from Arnorsson (2000)

	H ₂ S/H ₂	H ₂	CO ₂ /H ₂	H ₂ S	CO ₂	AVE	STDEV
AB-19-G04				250	418		
AB-19-G05				266	541		
AB-19-G06				271	576		
AB-19-G02	249	229	144	208	501	266	122
AB-19-G04	247	229	158	208	428	254	92
AB-19-G06	226	225	128	224	564	273	150

2.4 Soil Flux Survey

Along the northwestern Abaya fault and especially where surface manifestations are observed a soil flux survey was conducted. Structures with temperature and gas flux anomalies, likely to originate in the geothermal reservoir, were targeted. These profiles are displayed in *Figure 10*.

After conducting geological and geochemical surveys in the area the soil gas and temperature survey was focused on the Salewa Dore - Hako graben (SD-H graben) and the Abaya spring area (location of the northwestern Abaya fault). The SD-H graben is characterised by large number of scoria cones and large central volcanic complex (Hako and Salewa Dore) located in the graben. The Abaya spring area is characterised by many surface manifestations in the form of fumaroles, springs and hydrothermally altered surface. The spring temperatures range from 40 °C to 100 °C and sound of vigorously boiling groundwater at shallow depths. Some of the springs have high gas flux.

Total of 757 points were measured. Due to the large area and limited surface manifestations, apart from the Abaya springs, the measuring points were laid out with 50 m interval, making the total flux profiles approx. 37 km. The profiles were laid out to try to cover large area crossing the dominant fault direction perpendicular. The station interval is 50 m and the area that is covered based on the 25 m radius is 1.49 km², but more conservative estimate is looking at active radius of 10 m.

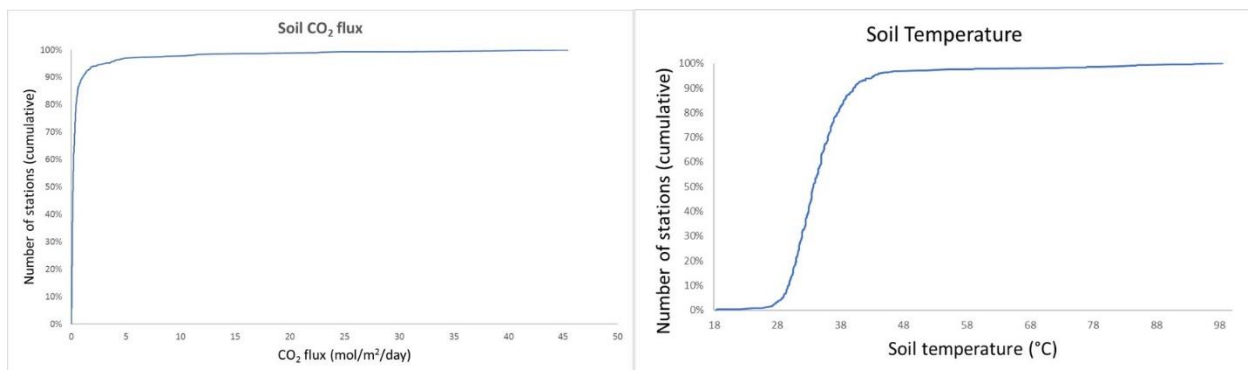


Figure 9. Cumulative graphs of the soil flux and soil temperature survey. The highest 75% values are considered to be influenced by geothermal source and the 10 % are considered to be of geothermal origin.

The values of the flux and temperature are split into three groups: background value is the lowest 75% of the measured values, 75-90% of the values are considered transitional or influenced by geothermal heat of gas flux and the highest 10% are considered to stem from geothermal activity. The temperature and flux values are listed in *Table 5*, and the cumulative diagrams displayed in *Figure 9*.

Table 5. The measured background, transitional and geothermal anomalies.

	Cumulative %	Temperature °C	Flux CO ₂ mol/m ² /day
Background	<75	< 36.7	<0.368
Transitional	75 - 90	36.7-40.1	0.368 - 1.017
Anomaly	90>	> 40.1	> 1.017

The anomalies within the study area are closely associated with the fault surface manifestations in the area as well as the eastern fault of the SD-H graben. The largest anomaly area is observed around the Abaya springs.

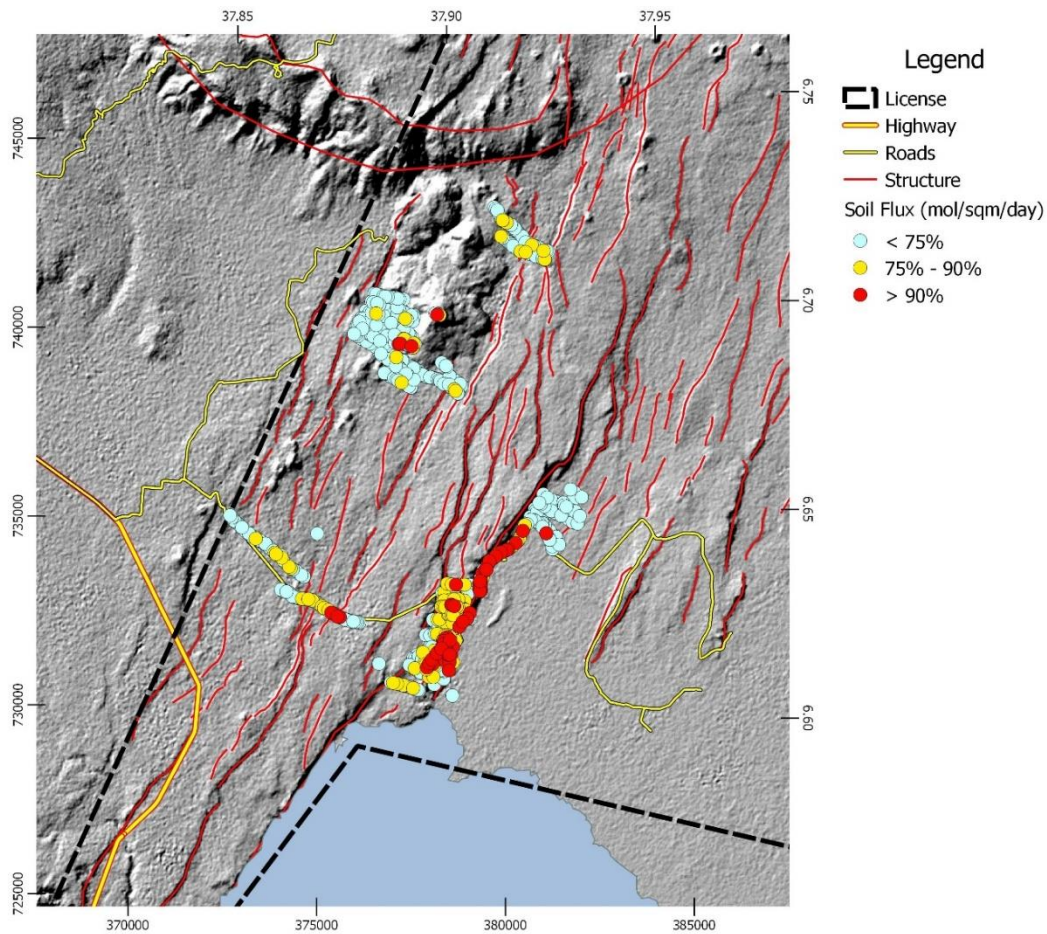


Figure 10: Spatial distribution of CO₂ soil flux in Abaya. Flux is reported in cumulative percentage, with blue circles representing a background value, yellow representing a transitional value and red representing a geothermal anomaly.

The temperature range at 50 cm soil depth is 18.3 – 98.5 °C and the temperature distribution of the collected data is shown on a cumulative graph in *Figure 9* where 90% of the points have temperature level lower than 40.1 °C and values below 36.7 °C, the 75% lowest values, are considered a background value. This temperature is also close to the atmospheric temperature in shade during the field days, and therefore are in good agreement to be considered natural values, i.e. not affected by geothermal heat flow. *Figure 11* shows spatial distribution of temperature at 50 cm depth for the measured profiles.

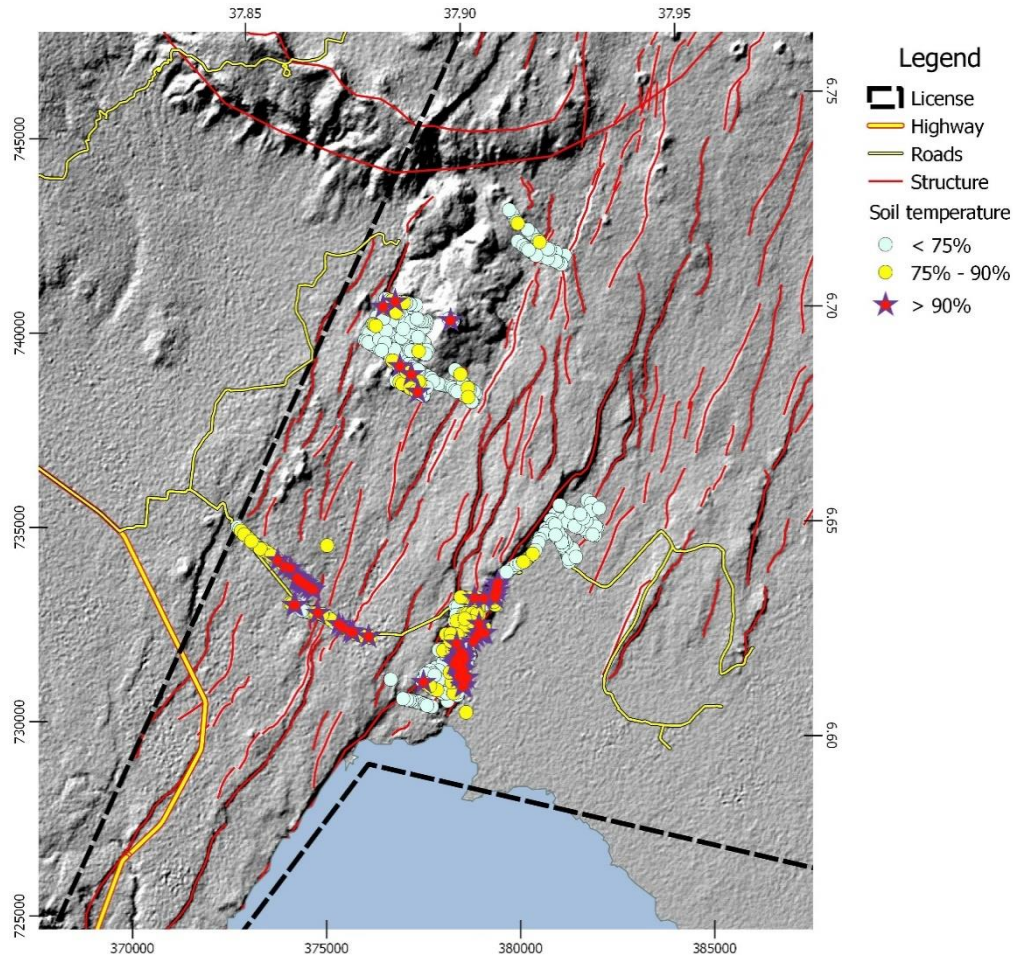


Figure 11. Temperature map of survey area, at 50 cm depth in the soil cover. Temperatures measurements are represented in cumulative percentage, with blue circles representing a background value, yellow representing a transitional value and red representing a geothermal anomaly.

There is a good agreement between the soil gas flux anomaly as well as the soil temperature flux anomaly, indicating an area with permeable structures that allows easy flow of geothermal fluids to the surface. The soil flux is also highest in areas where the surface manifestations are located.

2.5 Resistivity

The resistivity exploration in Abaya was conducted between December 2018 and March 2019. 88 TEM and 81 MT soundings were done in the area. The first interpretation of the TEM data indicate the presence of a low resistivity structure at several hundred meters below the surface that likely indicates a clay cap, *Figure 12*. The MT data has not been interpreted as of March 14th, 2019.

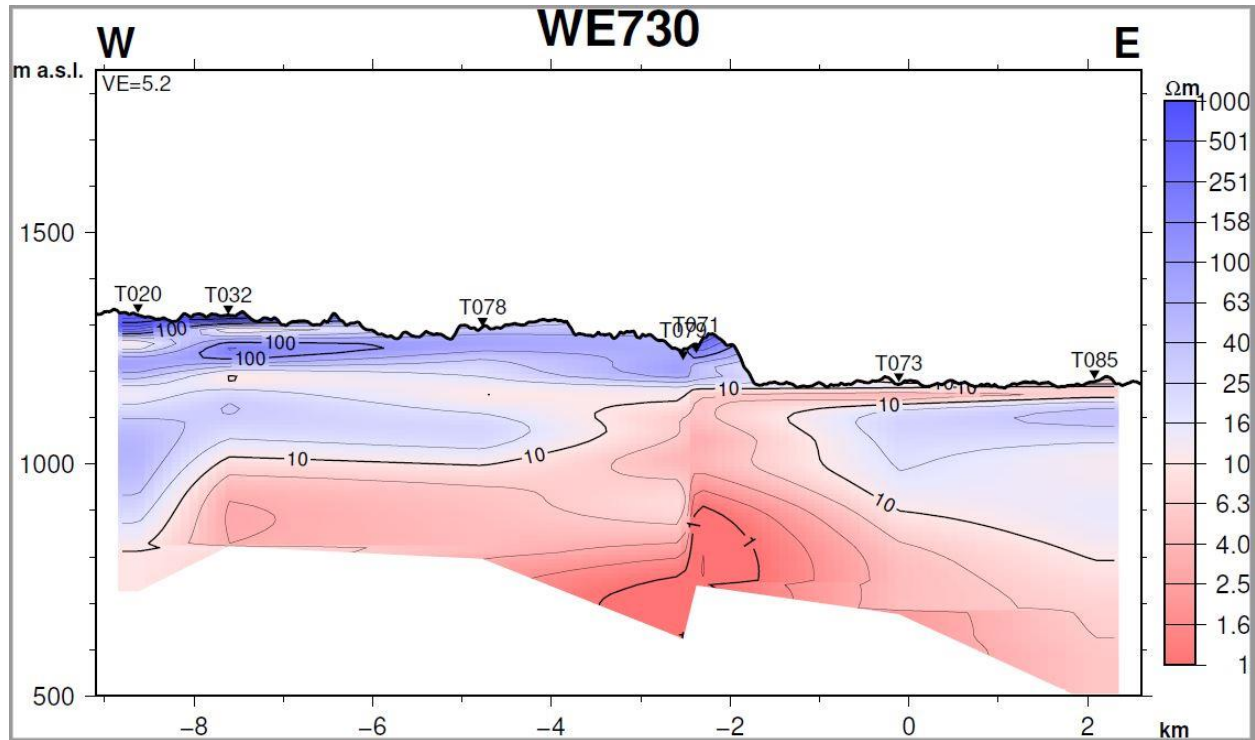


Figure 12. Resistivity profile, from W to E (profile A in Figure 4). This shows an indicated top of a clay cap at several hundred-meter depth.

3. Conclusion

The Abaya geothermal prospect has been studied extensively by Reykjavik Geothermal. The overall geological structure presents surface thermal manifestations hosted by permeable fault systems, as indicated by thermal springs, altered ground and confirmed further from the results of soil-flux analysis. The fluid chemistry analysis indicates fluids sources derived from a geothermal reservoir, with geothermometer measurements suggesting temperatures greater than 200 °C. The results from MT/TEM surveying of the area present the presence of a clay cap very close to the surface, at a few hundred meters of depth. All of these combined factors strongly suggest the presence of a high-enthalpy reservoir suitable for geothermal power production.

Acknowledgements

The surface exploration has been carried out with grant from the Geothermal Risk Mitigation Fund (GRMF). A good collaboration with Addis Ababa University and University of Iceland with field work and independent student projects.

REFERENCES

- Arnorsson, S. (2000). *Isotopic and chemical techniques in geothermal exploration, development and use. Sampling methods, data handling, interpretation.* (S. Arnorsson, Ed.). Vienna: International Atomic Energy Agency.
- Ayele, A., Teklamariam, M., & Kebede, S. (2002). *Geothermal Resource Exploration in the Abaya and Tulu Moye-Gedemsa Geothermal Prospects, Main Ethiopian Rift: Part II Abaya Geothermal Prospect.* Addis Ababa.
- Chernet, T. (2011). Geology and hydrothermal resources in the northern Lake Abaya area (Ethiopia). *Journal of African Earth Sciences*, 61(2), 129–141. <https://doi.org/10.1016/j.jafrearsci.2011.05.006>
- Corti, G., Sani, F., Philippon, M., Sokoutis, D., Willingshofer, E., & Molin, P. (2013). Quaternary volcano-tectonic activity in the Soddo region, western margin of the Southern Main Ethiopian Rift. *Tectonics*, 32(4), 861–879. <https://doi.org/10.1002/tect.20052>
- Di Paola, G. M. (1970). *Geological-geothermal report on the central part of the Ethiopian Rift Valley.* Addis Ababa.
- Electroconsult (ELC). (1987). *Geothermal reconnaissance study of selected sites of Ethiopian Rift Systems (Geological Report).* Milan.
- Fournier, R. O. (1977). Chemical geothermometers and mixing models for geothermal systems. *Geothermics*, 5(1–4), 41–50.
- Giggenbach, W. (1988). Geothermal solute equilibria. derivation of Na-K-Mg-Ca geothermometers. *Geochimica et Cosmochimica Acta*, 52(12), 2749–2765.
- Mamo, T., & Abteu, Z. (2008). *Ministry of Mines and Energy: Report on Surface Temperature Measurements In Abaya Geothermal Prospect.* Addis Ababa.
- Minissale, A., Corti, G., Tassi, F., Darrah, T. H., Vaselli, O., Montanari, D., ... Teclu, A. (2017). Geothermal potential and origin of natural thermal fluids in the northern Lake Abaya area, Main Ethiopian Rift, East Africa. *Journal of Volcanology and Geothermal Research*, 336, 1–18. <https://doi.org/10.1016/j.jvolgeores.2017.01.012>
- Mohr, P. A. (1971). Ethiopian rift and plateaus: Some volcanic petrochemical differences. *Journal of Geophysical Research*, 76(8), 1967–1984.